HGGA, Volume *4*

Supplemental information

Biallelic pathogenic variants in the mitochondrial form of phosphoenolpyruvate carboxykinase cause peripheral neuropathy

Neal Sondheimer, Alberto Aleman, Jessie Cameron, Hernan Gonorazky, Nesrin Sabha, Paula Oliveira, Kimberly Amburgey, Azizia Wahedi, Dahai Wang, Michael Shy, and James J. Dowling.

Supplement

Supplemental material and methods

Patient information

Written informed consent was obtained from all study participants via an REB approved protocol (Dowling REB#: 1000009004, Hospital for Sick Children, REB#: 1000009004). Commercial whole exome sequencing was performed at GeneDx. Nerve conduction studies were performed as part of routine clinical care (Gonorazky, Hospital for Sick Children).

Patient variants
Subject P.1 has PCK2 variants c.68C>G; p.S23X (ClinVar ID 374449) and c.509C>T; p.P170L (ClinVar ID pending). Subjects P. 2-1 and P. 20-2 are homozygous for the PCK2 variant c.577C>T; p.R193X (ClinVar ID 451808).

Patient fibroblast studies

Fibroblasts were obtained from the palmar surface of the distal upper extremity. Local anesthetic was used for pain control. Cultures were established at the diagnostic resource centre (Hospital for Sick Children), and then experiments were performed on early passage cells.

Mouse line details

The mouse line C57BL/6N-Pck2<em1(IMPC)Tcp>/Tcp was made as part of the KOMP2-Phase2 project (https://www.mousephenotype.org/) and generated at The Centre for Phenogenomics . It was obtained from the Canadian Mouse Mutant Repository.

Mouse nerve conduction studies

Nerve conduction studies were performed as per Schulz et al (2014) with minor modifications. Mice were anesthetised with 3% isoflurane/100% oxygen by inhalation for initiation of anesthesia and then maintained on 2% isoflurane/100% oxygen for the procedure. For stimulation and recording, we used a portable electromyography unit (Nicolet VikingQuest System, WI USA) and subdermal needle electrodes of 13 mm length. Compound muscle action potentials were recorded from the gastrocnemius muscle after stimulation of the sciatic nerve (see Supplemental Figure 3).

Mouse nerve pathology assessment

Sciatic nerves from knockout (n = 8) and wild type (n = 6) animals were dissected and immediately place at 4°C in EM fixative (4% paraformaldehyde, 2% glutaraldehyde containing 0.1 M sodium cacodylate buffer). Samples were incubated overnight, then taken to the Advanced Bioimaging Center (The Hospital for Sick Children), where they

were dehydrated and then embedded for sectioning. Semi-thins sections were cut and stained with toluidine blue. Micrographs were captured with an Infinity1 camera (Lumenera Corporation, Ottawa, CA) with CellSens Standard software visualized through an Olympus BX43 light microscope (Olympus, Center Valley, PA). Three different fields per slide were photographed, using 200x magnification.

For quantification, images were prepared using ImageJ Fiji software (Rasband, 1997-2018), starting with setting the scale and transforming the image to 8-bit. They were then segmented using AxonSeg (Zaimi A, 2016). Using this software, we first determined manually the pixel size, the threshold of axon segmentation, and axon discrimination parameters (minimal size, solidity and ellipticity). The same parameters were used on all images. Checking of segmentation was done after processing, and segments were removed or added manually. After setting the parameters, relevant morphometric data were automatically extracted, with the software calculating myelin thickness, myelin area, axon area, and axon diameter, and then generating a table with all data that can be opened using Matlab (Natick, 2021).

Using Excel (Microsoft Corporation, 2018. Microsoft Excel), the data obtained from the 3 fields was added to calculate average axon diameter distribution, axon density and the myelin thickness distribution. Analyses of each parameter in order to evaluate statistical significance were made using GraphPad Prism version 9.1.2 for Windows (GraphPad Software, San Diego, California USA, www.graphpad.com).

References

Natick, M. T. (2021). MATLAB. version R2021a.

Schulz, A., Walther, C., Morrison, H., Bauer, R (2014). In Vivo Electrophysiological Measurements on Mouse Sciatic Nerves. J. Vis. Exp. (86), e51181.

Rasband, W. (1997-2018). ImageJ. *National Institutes of Health, Bethesda, Maryland, USA*. Retrieved from https://imagej.nih.gov/ij

Zaimi A, D. T.-A. (2016). AxonSeg: Open Source Software for Axon and Myelin Segmentation and Morphometric Analysis. *Front Neuroinform*, 10:37. doi:10.3389/fninf.2016.00037

Supplemental figures and tables

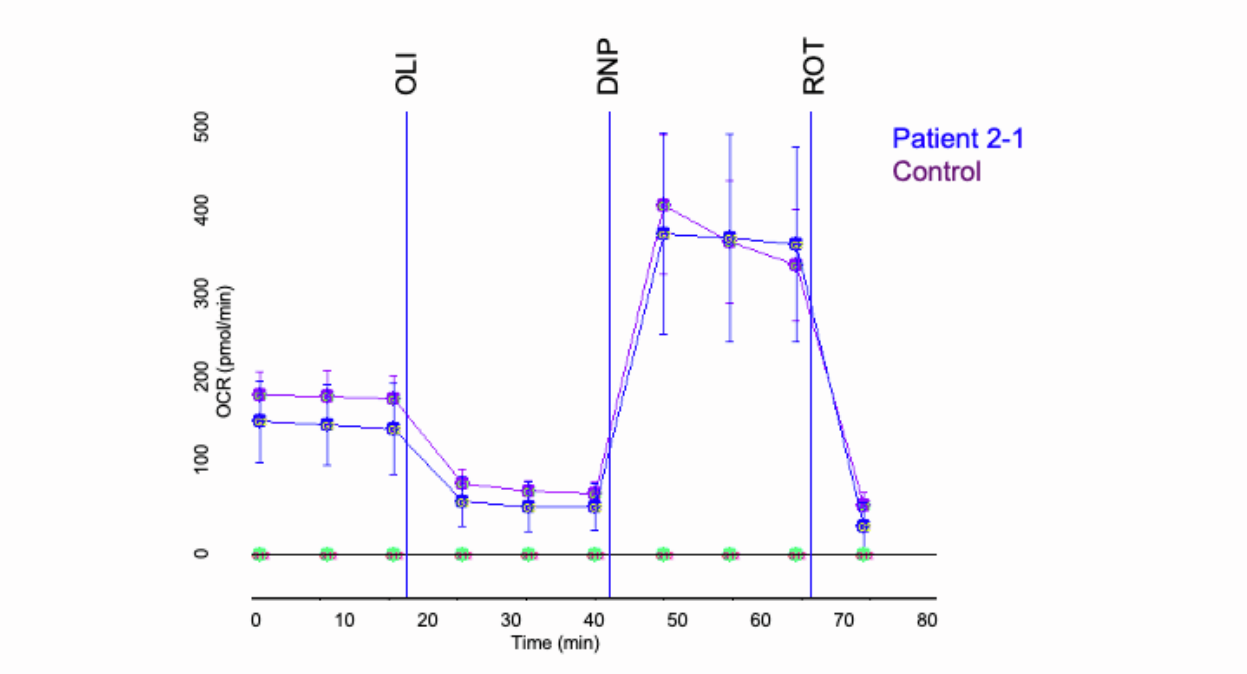

Figure S1 Oximetry of patient fibroblasts
Oximetry studies were performed using intact fibroblasts from P. 2-1 and an unrelated control. Oligomycin (OLI), dinitrophenol (DNP) and rotenone/antimycin A (ROT) were added at the indicated times. Analysis, quantitation and statistics were performed on an XF-96 oximeter (Seahorse). There were no significant differences at any time point.

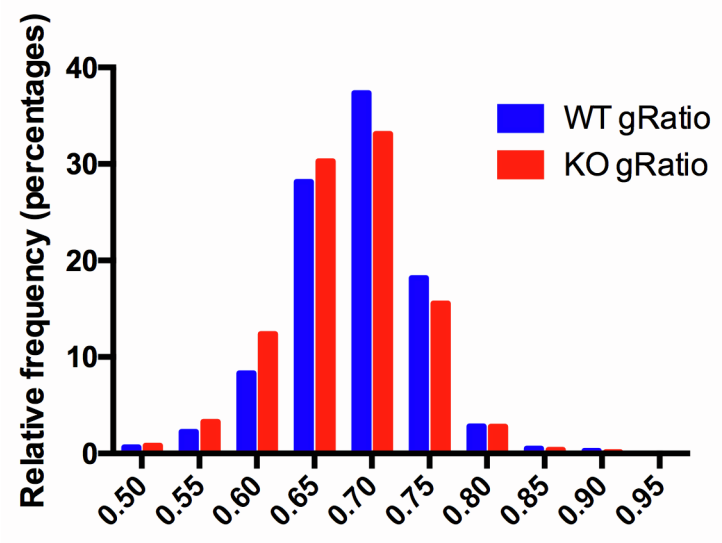

Figure S2: Abnormal g ratios in *Pck2* knockout sciatic nerves.
Sciatic nerves were dissected, processed, cut as semi thin sections, and then evaluated under light microscopy. Axon diameter, myelin sheath diameter, and the inner-to-outer sheath distance were all obtained. G ratios were calculated for all nerves. The g ratio (r/R) is the ratio between the inner and outer diameters of the myelin sheath, and is computed from the axon volume fraction (r) and the nerve (axon + myelin) volume fraction (R). G ratios were shifted to the left in knockout nerves, representing thinner myelin sheaths per axon diameter. ($p = 0.00001$).

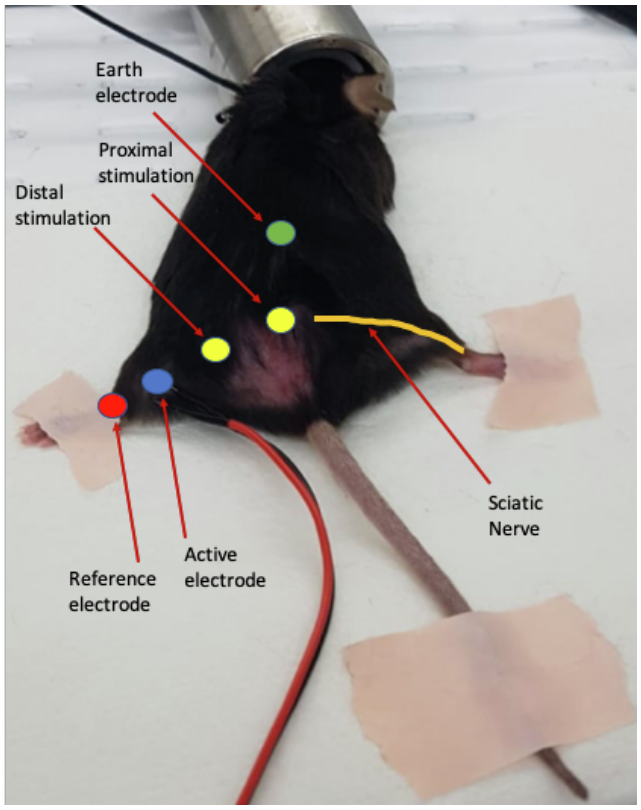

Figure S3: Sciatic motor nerve conduction velocity (NCVs) analyses. Measurement of electrophysiological responses of the sciatic nerve *in vivo* with the different positions of the electrodes used (adapted with minor changes from Schulz et al, 2014). Recording was done over gastrocnemius muscle (blue), with additional electrodes at reference (red) and ground/earth (green) sites. Stimulation was performed using needle electrodes at defined positions for proximal and distal stimulation sites (yellow). The orange line shows the approximate location of the sciatic nerve.

Table S1

A. Patient 1.1

Nerve stimulated	Site stimulation	Distal latency (m/s)	Amplitude (Motor=mV - Sensory=uV)	Conduction velocity (m/s)	F-wave Latency ms
L median (S)	Wrist	NR			
R ulnar (S)	Wrist	NR			
L superficial peroneal (S)	Leg	1.79	11.2	39.1	
R sural (S)	Calf	NR			
	Wrist	3.58	5.2		
R median (M)	Elbow	8.79	3.2	46.1	
	Wrist	3.16	4.1		
L ulnar (M)	Ab elb	9.56	4.8	37.5	
	Ankle	3.87	1.55		
R peroneal	Ab knee	13.8	0.76	34.2	
	Ankle	4.55	1.17		
L peroneal	Ab knee	13.0	0.39	36.5	
	Ankle	5.79	3.6		
L tibial	Knee	15.8	2.6	38.0	61.5
	Ankle	3.93	2.5		
R tibial	Knee	15.4	0.79	31.1	

B. Patient 1.2

Nerve stimulated	Site stimulation	Distal latency (m/s)	Amplitude (Motor=mV - Sensory=uV)	Conduction velocity (m/s)	F-wave Latency ms
L median (S)	Wrist	2.04	23,0	49.0	
L ulnar (S)	Wrist	1.50	12.1	50.0	
L superficial peroneal (S)	Leg	NR			
R sural (S)	Calf	NR			
	Wrist	3.77	4.7		
L median (M)	Elbow	10.2	4.2	38.9	
	Wrist	4.01	5.1		
L ulnar (M)	Ab elb	10.7	3.0	38.8	
	Ankle	6.70	0.80	28.9	
L tibial	Knee	20.2	0.42		NR
	Ankle	6.08	1.31		
R tibial	Knee	20.4	0.54	30.7	

N: No Response; R: right; L: left; S: sensory; M: motor.

Table S1. Nerve conduction studies from PCK2 patients.
Nerve conduction studies from two siblings with biallelic *PCK2* pathogenic variation. In both cases, the nerve conduction study showed primarily sensory-motor demyelinating length-dependent polyneuropathy. There was also evidence of temporal dispersion in some nerves, as well as important asymmetry in velocities and amplitudes.

	Genotype	Gender	Sciatic nerve (side)	Distal CMPA amplitude (mV)	Proximal CMPA amplitude (mV)	Temporal dispersion	Conduction velocity (m/s)
			R	37,5	29,8		40,0
1	KO	M	L	14,5	12,5		47,1
			R	27,4	26,6		58,7
2	KO	M	L	22,2	23,0		52,9
			R	44,7	58,7		58,0
3	KO	M	L	67,6	61,3		64,7
			R	16,6	14,0		16,0
4	KO	M	L	16,7	30,5		38,0
			R	17,9	21,4		32,0
5	KO	F	L	22,1	24,1		26,0
			R	25,0	20,4		36,0
6	KO	M	L	5,1	4,6	Present	37,0
			R	9,7	10,5		62,0
7	KO	M	L	23,1	21,7		96,0
			R	14,2	11,5		54,0
8	KO	M	L	7,7	7,7		58,0
			L	18,1	20,5		61,0
9	KO	F	R	11,2	21,2		72,0
			L	29,9	29,4		41,0
10	KO	F	R	24,7	26,3		38,0
			L	19,8	11,5		33,0
11	KO	F	R	9,7	14,9		36,0
			L	18,5	26,6		83,0
12	KO	F	R	25,0	27,0		36,0
			R	18,3	15,2		82,0
13	KO	F	L	24,1	29,4		96,0
			R	22,6	21,8		62,0
14	KO	F	L	17,0	21,0		67,0
			R	15,3	15,6	Present	35,0
15	KO	F	L	24,9	28,5		42,0
			R	23,4	20,3		62,0
16	WT	F	L	18,3	22,9		72,0
			R	47,3	49,9		58,8
17	WT	M	L	34,3	24,3		56,3
			R	7,9	8,0		64,0
18	WT	M	L	16,0	30,0		38,0
			R	12,8	21,1		32,0
19	WT	F	L	24,5	22,5		34,0
			R	16,1	18,0		70,0
20	WT	F	L	19,3	18,8		35,0
			R	7,1	7,5		91,0
21	WT	M	L	11,1	10,6		105,0
			R	15,6	15,6		87,0
22	WT	M	L	18,5	23,3		104,0
			R	34,3	33,8		82,0
23	WT	M	L	22,3	21,1		47,0
			R	15,3	13,4		67,0
24	WT	M	L	14,0	11,1		38,0
			L	16,7	28,9		83,0
25	WT	F	R	22,7	26,1		65,0
			R	12,3	14,0		41,0
26	WT	F	L	13,5	11,8		41,0
			R	19,4	18,5		62,0
27	WT	F	L	40,7	43,1		67,0
			R	18,9	17,7		46,0
28	WT	F	L	13,4	14,3		48,0
			R	15,6	25,2		83,0
29	WT	F	L	11,9	17,3		83,0
			R	20,0	24,9		53,0
30	WT	F	L	10,1	8,9		53,0

KO: Knockout; WT: wilde type; M: male; F: female; R: right; L: left.

Table S2. Mouse sciatic nerve motor conduction values.

Individual compound muscle action potential (CMAP) amplitudes and sciatic nerve conduction velocities for all mice in the study (n = 15 per group, *Pck2* knockout = KO and wild type = WT). Note that temporal dispersion, a sign of demyelination, was only seen in

KO mice. Additionally, 6/15 KO mice had reduced conduction velocities (defined as velocity < 40 m/s), while only 1/15 WT had reduced velocities.